# Entropy Waves Produced in Oscillatory Combustion of Solid Propellants

H. KRIER* AND M. SUMMERFIELD†
*Princeton University, Princeton, N. J.*
AND
H. B. MATHES‡ AND E. W. PRICE§
*Naval Weapons Center, China Lake, Calif.*

**The dynamic response of a flat solid-propellant flame to an oscillating pressure field was studied experimentally in a window burner fitted to a T-tube rocket motor that served as a pressure oscillator. The burned gas temperature was measured as a function of time (or phase) during a pressure oscillation, and also as a function of distance from the surface. Such instantaneous measurements of gas temperature, when coordinated with simultaneous measurements of pressure, provide a measure of the entropy content of each element of gas as it flows away from the flame. Since the entropy content of each element of gas is nearly conserved as it flows along, an entropy wave train is formed. It is possible to make deductions regarding the physics of the dynamic burning process by comparing the magnitude and phase of the observed entropy waves with the theoretical values predicted on the basis of a particular flame model. In general, the results show that the temperature of the gas flowing from the combustion zone responds neither isentropically nor isothermally to the pressure. Such responses were assumed in previous publications on the subject. However, on the basis of the KTSS model published recently, the magnitude and phase of the entropy wave are expected to vary in a more complicated form with the imposed frequency and the propellant properties. The observed waves reported in this paper tend to support these KTSS theoretical expectations.**

## Nomenclature

$A$ = dimensionless pyrolysis exponent, as defined in Ref. 7
$c$ = specific heat, cal/g °K
$E$ = term defined by Eq. (24) of Ref. 6
$H$ = dimensionless heat release at the propellant surface, $[Q_s/c(\bar{T}_s - T_\infty)]$
$m$ = power of propellant pyrolysis law, $[r = b(T_s - T_\infty)^m]$
$n$ = pressure index in steady burning relation, $[\bar{r} = ap^n]$
$p$ = pressure, kg/cm$^2$ (or psi)
$r$ = burning rate of propellant, cm/sec
$\mathcal{R}$ = universal gas constant, cal/g-mole °K
$s$ = entropy of burned gas, cal/g °K
$t$ = time, sec
$T$ = temperature, °K
$u$ = gas velocity, cm/sec
$x$ = dimension (from flame zone), cm
$Y$ = acoustic admittance, as defined in Eqs. (1) and (2)
$\alpha$ = thermal diffusivity of the solid, cm$^2$/sec; also stability parameter as defined in Ref. 7
$\gamma$ = ratio of specific heats of burned gas
$(\Delta P)$ = dimensionless amplitude of pressure oscillation
$(\Delta S)$ = dimensionless amplitude of entropy oscillation, as defined in Ref. 6
$\xi$ = $(\bar{T}_s - T_\infty)/\bar{T}_f$
$\omega^*$ = frequency, rad/sec
$\omega$ = dimensionless frequency, $[\omega^*(\alpha/\bar{r}^2)]$
$\theta$ = dimensionless temperature, $[(T - T_\infty)/(\bar{T}_s - T_\infty)]$
$\tau$ = dimensionless time, $[t/(\alpha/\bar{r}^2)]$
$\psi$ = phase angle between perturbed pressure and surface temperature [defined in Eq. (24) of Ref. 6]
$\phi$ = phase angle between experimental pressure and temperature oscillation

### *Subscripts*

$g$ = gas
$s$ = solid surface
$f$ = flame (burned gas)
$\infty$ = ambient solid

### *Superscripts*

$(\bar{\ })$ = steady-state value; mean value
$(\ )'$ = perturbed value

Presented as Paper 68-499 at the ICRPG/AIAA 3rd Solid Propulsion Conference, Atlantic City, N. J., June 4–6, 1968; submitted June 4, 1968; revision received May 12, 1969. Based on work performed under Contract AF 49(638)-1405 at Princeton University and parallel research at the Naval Weapons Center.

* Postdoctoral Research Associate; now Assistant Professor, University of Illinois. Member AIAA.
† Professor of Aerospace Propulsion. Fellow AIAA.
‡ Physicist, Aerothermochemistry Group. Member AIAA.
§ Head, Aerothermochemistry Group. Associate Fellow AIAA.

## I. Introduction

KNOWLEDGE of the response of propellant combustion processes to flow perturbations is vital to any quantitative description of acoustic instability. The nature of this dynamic coupling between the flame zone and the gas dynamic environment has been the basis of numerous theoretical and experimental investigations aimed at determining the acoustic admittance of a burning propellant, its extinguishment characteristics under sudden depressurization, and its other response characteristics. The acoustic admittance appears as a boundary condition in the solution of the wave equation and it describes the flow of energy into or out of the acoustic wave. The admittance is defined as

$$Y = -u'/p' \tag{1}$$

where $u'$ is a velocity perturbation normal to the propellant surface and $p'$ is a pressure perturbation. When written in terms of variables related to propellant combustion, the

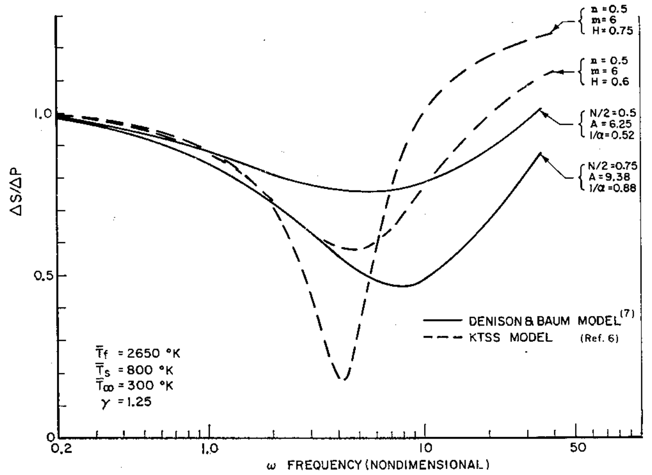


**Fig. 1 Amplitude of entropy wave at edge of flame: comparison of KTSS and DB models.**

admittance becomes[1]

$$Y = -(\bar{u}/\bar{p})\{\mu/\epsilon - \sigma/\epsilon\} \tag{2}$$

where $\bar{u}$ is the mean gas velocity, $\bar{p}$ is the mean pressure, $\mu/\epsilon$ is the dimensionless ratio of the mass perturbation to the pressure perturbation, and $\sigma/\epsilon$ is the ratio of the density perturbation to the pressure perturbation. It is assumed that these quantities are calculated at a plane near the propellant surface but at a location outside the chemical reaction zone. It is further assumed that the fluctuations of gas velocity and pressure correspond to a standing acoustic wave mode, that the flame zone thickness is small compared to the acoustic wavelength and to the other dimensions in the system, and that the gas-phase reaction time is short compared to the period of acoustic oscillation and also to the relaxation time of the thermal wave in the subsurface region of the solid. It should be noted that, in general, $Y$ is a complex quantity, that is, the velocity response to a pressure perturbation must be described by a phase angle as well as a magnitude. However, the real part of the complex admittance determines whether or not an acoustic wave will be amplified; the out-of-phase (or imaginary) component of the velocity response cannot amplify a pressure perturbation.

The ratio $\mu/\epsilon$ is commonly referred to as the "response function" and considerable theoretical and experimental investigation has been devoted to determining its magnitude and phase.[2-4] The magnitude of the response function, according to T-burner results, typically falls in the range between unity and 5. Less emphasis has been put on evaluating $\sigma/\epsilon$, the density response function, since theoretical studies indicate that it is of the order of unity in magnitude. This ratio, in addition to $\mu/\epsilon$, is sensitive to the nature of the processes in the over-all combustion zone. If the density of the gas emerging from the combustion zone were thought to respond to the pressure isentropically, $\sigma/\epsilon = 1/\gamma$. The ratio would equal unity if the density were to respond isothermally; but for actual flames this ratio will assume some other value that depends on the flame structure and the frequency of oscillation. Knowledge of the density response ratio, or of its equivalent, the temperature response ratio, therefore, provides an excellent diagnostic test of flame structure theory.

The earliest published analysis of the acoustic admittance of a solid propellant[1] was based on the mistaken assumption that $\sigma/\epsilon$ is isentropic. Shortly afterward this assumption was questioned, and then experiments to measure the degree of nonisentropicity were initiated.[5] Unfortunately, the first attempts to verify nonisentropic behavior during pressure oscillation were either negative or inconclusive.[5] Recent theoretical studies,[6] however, indicated that these experiments may have failed to verify nonisentropic behavior because they were conducted at frequencies ill-suited for displaying the phenomenon.

## II. Entropy Waves

As mentioned previously, the term $\sigma/\epsilon$ is the variation of density with pressure, as seen by an observer stationed at the outer edge of the flame zone. If the relationship is represented by a polytropic formula for convenience (perfect gas law), the density variation can be expressed in terms of the variations of the entropy of the burned gas with pressure, or alternatively, in terms of the temperature fluctuation. That is,

$$\begin{aligned}\sigma/\epsilon &= 1/\gamma + (1/c)(ds_f/d\ln\rho) \\ &= (1/\gamma)(1 + \zeta/\epsilon) \end{aligned} \tag{3a}$$

where

$$\zeta = [(\gamma - 1)/\gamma]p'/\bar{p} - T'_f/\bar{T}_f \tag{3b}$$

The temperature is meaningful only if its variation is observed in coordination with the pressure variation. If this is done, it is preferable to report the combined effect of temperature and pressure as an entropy value, since, as each element of the combustion gas travels away from the flame zone into the acoustic field, its temperature and pressure vary with time, but its entropy remains nearly constant (except at high frequencies and short wavelengths when heat diffusion becomes important). Then assuming that the gas behaves isentropically *after* it leaves the combustion zone, the subsequent state of each element of gas is given in terms of its state when it left the combustion zone by the relation

$$\frac{T(x,t)}{T(0,t - x/\bar{u})} = \left[\frac{p(x,t)}{p(0,t - x/\bar{u})}\right]^{(\gamma-1)/\gamma} \tag{4}$$

where $\bar{u}$ is the mean velocity of a given gas particle. $T(x,t)$ is the gas temperature at time $t$ at observation station $x$, while $T(0,t - x/\bar{u})$ is the flame temperature of the same element of gas at time $t - x/\bar{u}$. The time retardation $x/\bar{u}$ is an approximation for the true value, which is

$$\int_0^x \frac{dx}{\bar{u} + u'\sin(\omega^* t)}$$

The approximation results in a slight distortion of the spatial wave form. Equation (4) can thus be used to describe a temperature wave that develops as a consequence of an entropy variation at the edge of the flame zone, $x = 0$. At that point the entropy is calculated with the relation

$$(s_f - \bar{s})/\mathcal{R} = [\gamma/(\gamma - 1)]\ln(T_f/\bar{T}_f) - \ln(p/\bar{p}) \tag{5}$$

The near constancy of the entropy of each element of burned gas as it moves downstream makes it a useful property to discuss theoretically and experimentally. We emphasize, however, that although the entropy of each element of burned gas remains constant with time, the entropy values of successive elements emerging from the flame are not the same but rather exhibit the wave structure implied by (4). This entropy variation of the gases at the edge of the flame zone has been shown to be of significance theoretically for interpreting the dynamic burning behavior of composite propellants.[6] Figure 1 shows the amplitude of predicted entropy perturbation $(s' - \bar{s})/\mathcal{R}$ at the flame, as a function of the nondimensional frequency $\omega$, from the theoretical analyses of Ref. 6 (KTSS model) and Ref. 7 (DB model). The value of $(\Delta S/\Delta P)$ depends critically on the combustion parameters of the solid and gas phase, namely, $m$, $H$, $A$, and $\alpha$. In general, $(\Delta S)$ is nonzero, i.e., the response is not isentropic. For very low frequencies of pressure oscillations, the behavior of the burned gas is nearly isothermal, and therefore $(\Delta S/\Delta P)$ approaches unity.

The variation of entropy from element to element shows up as an entropy wave train carried along with the burned gas stream. The entropy wave system will show the same frequency as the acoustic wave system, but the entropy wavelength will be determined by the mass velocity (say, $10^2$ cm/sec), whereas the acoustic wavelength will be determined by the velocity of sound (about $10^5$ cm/sec). Thus, the two wave systems will have lengths in the ratio of the order of 1000 to 1, as depicted in Fig. 2.

Of course, there are dissipative actions tending to smooth out the entropy variations so that the entropy fluctuations decay as they propagate away from the flame. The damping length is quite large[4,5] if only ordinary thermal conduction is accounted for; the local influence of viscous stress is even less important. However, turbulent flow conditions or large scale circulation can readily effect a decay.

Since entropy variations are detected experimentally as temperature fluctuations, it is important to express the spatial distribution of the temperature of the combustion gas as a function of time as it leaves the flame layer during a pressure oscillation. We consider the one-dimensional end-burning rocket motor. With the assumption that longitudinal heat conduction and mixing along the gas stream are negligible, and if the distance from the flame to the observation station is small compared to the acoustic wavelength, then

$$T(x,t) = \left[\frac{p(t)}{p(t - x/\bar{u})}\right]^{(\gamma-1)/\gamma} \cdot T_f\left(0, t - \frac{x}{\bar{u}}\right) \quad (4a)$$

i.e., the oscillations of each element of gas are isentropic.

Considering small oscillatory perturbations,

$$p = \bar{p} + p'; \quad T = \bar{T}_f + T'; \quad p'/\bar{p} = (\Delta P)\sin(\omega^* t)$$

Then, to first order

$$\frac{T'(x,t)}{\bar{T}_f} = (\Delta P)\,\frac{\gamma - 1}{\gamma}\left[\sin(\omega^* t) - \sin\left(\omega^* t - \frac{\omega^* x}{\bar{u}}\right)\right] + \frac{T_f'(0, t - x/\bar{u})}{\bar{T}_f} \quad (6a)$$

or in a clearer form

$$\frac{T'(x,t)}{\bar{T}_f} = (\Delta P)\cdot\frac{\gamma - 1}{\gamma}\left[2\sin\left(\frac{\omega^* x}{2\bar{u}}\right)\cos\left(\omega^* t - \frac{\omega^* x}{2\bar{u}}\right)\right] + \frac{T_f'(0, t - x/\bar{u})}{\bar{T}_f} \quad (6b)$$

where $\omega^*$ is the dimensional frequency in radians/sec.

For an isothermal flame response, i.e., $T'_f = 0$, maxima in the temperature fluctuation would be found at locations given by

$$\omega^* x/2\bar{u} = (k + \tfrac{1}{2})\pi \quad (7)$$

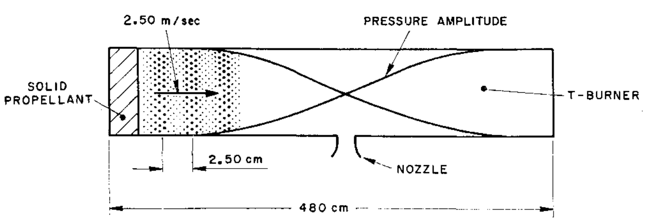


| | ENTROPY WAVES | ACOUSTIC WAVES |
|---|---|---|
| FREQUENCY | 100 cps | 100 cps |
| VELOCITY | 2.50 m/sec | 960 m/sec |
| WAVE LENGTH | 2.50 cm | 960 cm |

**Fig. 2 Entropy wave properties in an acoustic field.**

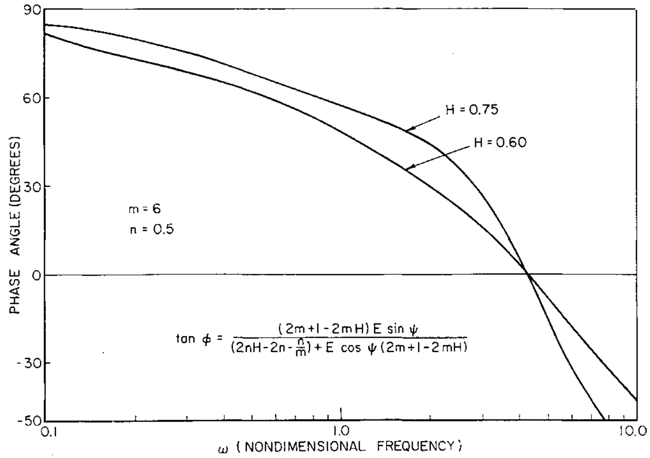


**Fig. 3 Phase angle of flame temperature with respect to pressure; calculated from the KTSS model.**

while the temperature fluctuation would be zero at points located at

$$\omega^* x/2\bar{u} = k\pi \quad (8)$$

where $k$ represents any positive integer, and $x$ represents the distance from the flame. Since during burning the propellant recedes from the initial observation point, $x$ is understood to be $(x_0 + \bar{r}t)$.

In order to predict the function $T'(x,t)$ for comparison with experiment, it is necessary to adopt a particular flame model in order to evaluate $T'_f(0,t)$ in Eq. (6b). We shall adopt the expression derived in Ref. 6 for diffusion-type flames[8] that describe the combustion of composite solid propellants. We have denoted it as the KTSS flame model.

Following the nomenclature of the KTSS model, the flame temperature perturbation is

$$\theta'_f = zP' + y\theta'_s \quad (9)$$

where

$$z = (2nH - 2n - n/m), \quad y = (2m + 1 - 2nH)$$

and the surface temperature perturbation is given by Eq. (24) of Ref. 6 as

$$\theta'_s = (\Delta P)E\cdot\sin(\omega\tau + \psi)$$

Both $E$ and $\psi$ are functions of frequency.

The flame temperature perturbation $T'_f$ equals $\xi\theta'_f$, and thus

$$T'_f/\bar{T}_f = (\Delta P)\xi G(\omega^*)\cdot\sin[\omega^* t + \varphi(\omega^*)] \quad (10)¶$$

where

$$G(\omega^*) = \{[yE\sin\psi]^2 + [z + yE\cos\psi]^2\}^{1/2}$$

$$\varphi(\omega^*) = \tan^{-1}\{yE\sin\psi/(z + yE\cos\psi)\}$$

and

$$E = E(\omega^*)$$

Finally, the desired gas temperature fluctuation $T'(x,t)$ can be expressed as

$$T'(x,t)/\bar{T}_f = (\Delta P)\{[(\gamma - 1)/\gamma][2\sin(\omega^* x/2\bar{u}) \times \cos(\omega^* t - \omega^* x/2\bar{u})] + \xi G(\omega^*)\sin[\omega^* t - \omega^* x/\bar{u} + \varphi(\omega^*)]\} \quad (11)$$

¶ At the limit of zero frequency ($\omega^* \to 0$), the flame temperature is 90° out of phase with the pressure. As the frequency is increased, this phase difference decreases, as shown in Fig. 3, which was plotted using Eq. (10). Near the "resonance" frequency of maximum solid phase temperature lag, the phase angle is zero, and the flame temperature amplitude is greatest.[9]

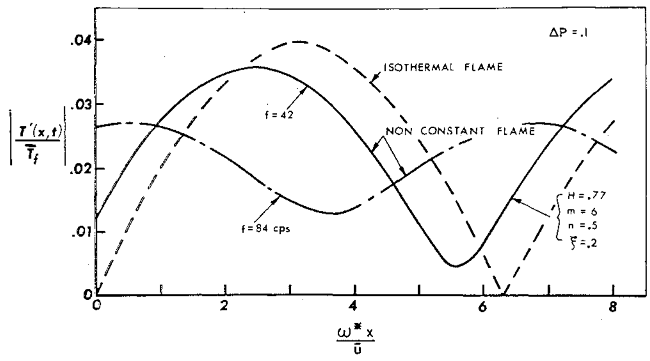


**Fig. 4 Amplitude of temperature wave as a function of distance from flame zone.**

This equation reveals that at any instant in time there would be a sinusoidal temperature variation in space; correspondingly, at any fixed observation point on the burner, there would be a sinusoidal variation of temperature with time. In addition, as shown in Fig. 4, if one were to observe the magnitude of the temperature fluctuations at various points along the burner, it would be found that the amplitude of temperature fluctuations varies with distance from the surface. Also, with a nonconstant flame temperature incorporated in the analysis, there will no longer be nodal locations in the temperature field, such as those specified for the isothermal flame case in Eq. (8).

Equation (11) provides a standard for comparing the foregoing theory with experimental observations. The observation of gas temperature variations as a function of space and/or time, coupled with knowledge of the acoustic frequency and the gas velocity, should be sufficient to test the existence of entropy waves. Sufficiently detailed knowledge of the relationship between the temperature fluctuations and the acoustic pressure would also permit one to determine the term $\sigma/\epsilon$ through the temperature response function given by Eq. (3b). It has recently been shown analytically, moreover, that entropy waves in a combustor sustaining $L^*$ combustion instability have a destabilizing effect at nonacoustic low frequencies.[10] The KTSS model was used to describe the dynamic burning rate perturbation for a given pressure perturbation in that analysis.

## III. Experimental Studies of Temperature Waves

Since the maximum spatial variation of the amplitude of the temperature fluctuations occurs when the flame responds isothermally (Fig. 4), it was decided that the initial oscillatory tests be made near to those conditions, in order to have the best chance of detecting these entropy waves. However, as discussed previously, this limiting behavior develops only for very low frequencies. The 5.5-in.-diam T-burner located at the Naval Weapons Center (NWC) was capable of operating in this frequency range,[11] and it was therefore decided to attempt to obtain evidence of nonisentropic behavior in that apparatus.

The burner is composed of several tubular sections that are bolted together to provide the desired length. The ends of the assembly are closed with caps which contain the propellant and means for ignition. The burner lengths ranged from 6 ft to over 60 ft, giving longitudinal mode frequencies from 250 cps down to 15 cps. An auxiliary air flow system is connected between the burner and nozzle to prepressurize the entire combustor before the start of burning. This avoids the need for burning an extra thickness of propellant to bring the combustor up to operating pressure. The air flow system serves also to control the burner pressure during the firing test by providing the major part of the gas flow through the nozzle.[11]

Two types of experiments were conducted: 1) a series in which photographic recording was utilized to obtain space-time records of the luminosity variation in the gas after it left the combustion zone; 2) a series in which high-speed temperature measurements were made at a fixed position using an adaption of the brightness-emissivity techniques. Three propellant compositions were used in the two series of tests: a) a bimodal polyurethane-AP composition (80:20) prepared at Princeton University (designated as PU) which contained 0.1% NaCl, b) a unimodal polyurethane-AP propellant (75:25) prepared at NWC (designated as A-152) which contained 0.4% NaCl, and c) a unimodal PBAN-AP propellant (76:24) prepared at NWC (designed as A-13).

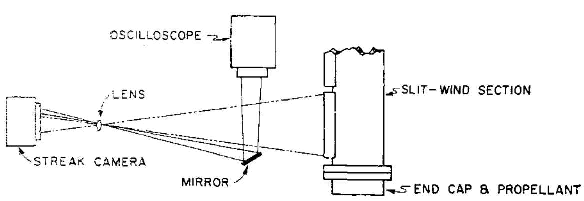


**Fig. 5 Block diagram of streak camera arrangement.**

### A. Streak Photographic Studies

The series of photographic experiments at NWC utilized a special burner section that was fitted with a nitrogen-flushed 6-in.-long slit window. An optical bench was used to mount a 70-mm streak camera and a long-focal-length objective lens. A cathode ray oscilloscope and mirror were arranged so that the oscilloscope screen was focused on the film plane in the camera in line with the image of the window slit. Thus, the acoustic pressure trace, which appeared on the cathode ray screen, was recorded simultaneously with the radiant intensity variations that appeared in the slit window of the burner. This arrangement permitted a detailed comparison to be made between events occurring in the burner gas and the acoustic pressure. A block diagram of the equipment arrangement used in the photographic studies is shown in Fig. 5.

A portion of the streak camera record is shown in Fig. 6. The photograph is typical of more than 15 tests obtained with the NWC burner in this range of low frequencies. The frequency of pressure oscillation was 120 cps, the mean burner pressure with 75 psia, the acoustic pressure amplitude was 9 psi peak-to-peak, and the time after ignition was approximately 2.3 sec. The acoustic pressure and approximate position of the propellant surface have been added to the figure as an aid in interpretation. Major features of interest have been inked onto the figure to the left of the photographic record for the same reason. The photographic portion of this figure is a positive, so that high- and low-temperature regions in the figure appear as light and dark areas respectively. Calculations from Eqs. (7) and (8), based on an estimate of the mean value of the burned gas velocity as it leaves the propellant flame, were made in order to predict the positions of the maximum and minimum temperature variations. These are designated in the figure as $T'$ max and

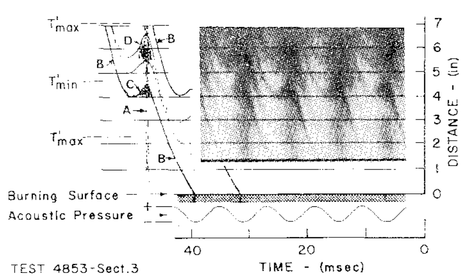


**Fig. 6 Portion of streak camera record from test with PU propellant using NWC burner.**

$T'$ min, respectively. Note also that a time and distance scale are provided in Fig. 6 and that time runs from right to left.

Major features in the reconstructed portion of the record are identified with letters as follows:

A) Period vertical darkened zones appear in the streak record at times when the acoustic pressure is a minimum. These dark low temperatures are related to the adiabatic cooling of the whole column of burned gas throughout the window section by lowering of the acoustic pressure at those times. (Note that there is also a general brightening at acoustic pressure maxima related to adiabatic heating from compression of gas in the burner by the acoustic wave.)

B) Dark diagonal lines, designated B, are relatively persistent in their travel across the section covered by the window. We interpret these to be elements of relatively cold gas that have originated from the propellant surface at a time when the acoustic pressure was a minimum. This assertion as to the origin of these elements of gas is derived from extrapolating the traces of the photographic record back to the propellant surface, as indicated in the inked reconstruction to the left of the photographic portion of the figure. It can be seen from this result that temperature oscillates in response to the pressure in such a way that, for the frequency of oscillation $\omega^*$, $T'_f/\bar{T}_f$ is nearly in phase with $p'/\bar{p}$. (It is clearly *not* a constant.) In view of the predictions of the KTSS theory (Fig. 1), this kind of response can be expected at $\omega$ greater than 10, which was the case here since $\bar{r}$ was fairly small at this low pressure.

C) Strong inflection points occur in the streak representing the motion of the gas elements (designated C). This suggests that the flow velocity actually reverses itself during some of the oscillation. It should be noted that the derivation described in Sec. II is based on small perturbations, and so it does not provide for a flow perturbation of the strength indicated in the record. One cannot expect, therefore, exact agreement between the theoretical prediction and experiment.

D) Dark areas, designated D, represent regions of cold gas, which at any instant in time occupy a position midway between B elements of gas. Since these appear between areas of gas (B designation) which originated at acoustic pressure minima, it seems probable that the D regions are related to the entropy fluctuations referred to in Eqs. (4–11).

Wave phenomena quite similar to the aforementioned have also been observed in the streak photographs of the combustion gas taken through a 4.5-in.-long slit window mounted on a 2.0-in.-diam T-burner at the Guggenheim Laboratories of Princeton University. The propellant was the same as that tested at NWC (PU designation). Figure 7 clearly shows the sinusoidal pattern of gas luminosity (somewhat distorted) superimposed on the dark and light temperature fluctuation, the latter caused by the isentropic compression and expansion of the gas column. The wavelength of the entropy waves (Fig. 2) for the conditions photographed in Fig. 7 was approximately $\frac{1}{2}$ inch.

There is the possibility that the temperature (and entropy) oscillations seen in the photographic streak records of Figs. 6 and 7 might have been produced by some physical or chemical factor other than the solid-phase heat lag described in theories such as those of Refs. 6 and 7. One such alternative mechanism is that the cyclic regression rates of binder and oxidizer are out of phase, which would imply a periodic fluctuation in the fuel-to-oxidizer ratio and hence an entropy wave.

One way to test the validity of this hypothesis would be to burn a homogeneous propellant (NG/NC) in a T-burner. If waves in the burned gas near the propellant surface are not

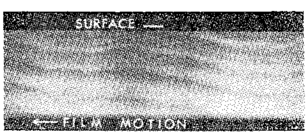


**Fig. 7 Portion of streak camera record using the Princeton burner in a test with PU propellant.**

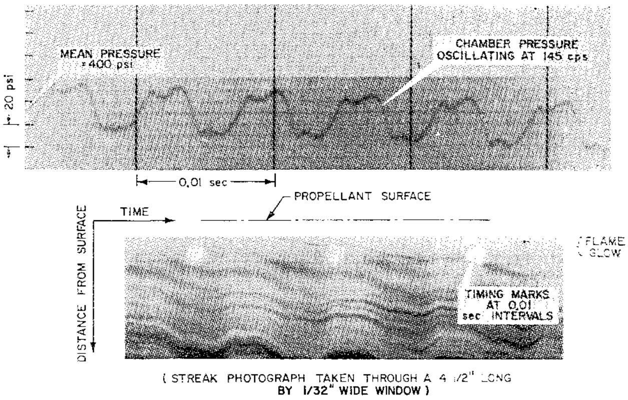


**Fig. 8 Pressure record and synchronized streak photograph of a double-base propellant near the burning surface.**

observed with a homogeneous propellant, then this mixture ratio oscillation phenomenon would have to be suspected as a cause of the waves photographed during the burning of a heterogeneous composite propellant. This test with a homogeneous propellant was recently made (using the Princeton 2.0-in.-diam T-burner) utilizing a standard ICRPG double base propellant, denoted as N-5. Figure 8 shows a streak photograph of one of the tests; the waves are indeed very similar to those observed with composite propellants. Since entropy waves were still detected for the homogeneous propellant, it seems unlikely that mixture-ratio waves cause the entropy waves seen with AP composite propellants.

### B. High-Speed Temperature Measurements (Optical Technique)

The second part of this investigation involved high-speed acquisition of gas temperature data from the gas column near the propellant surface. The temperature of flame gases is best measured by optical means, since no disturbance occurs, as it would from probes inserted in the flow. To make the variations in the temperature more marked, the flames were colored by sodium introduced by the addition of small amounts of sodium chloride to the test propellant. A brightness-emissivity method was used in the region of the D lines to determine the instantaneous temperature. It was assumed that thermal equilibrium of the sodium atom emitters with the all-burned combustion gases exists; this is a reasonable assumption since the zone of interest is outside the active reaction region.

This optical method utilizes the radiation only in a narrow spectral interval of about 120 a.u. straddling the D lines. The D lines at these conditions are 90 a.u. wide. Flame temperatures are calculated from variations in radiation intensity produced by light transmitted intermittently from a tungsten lamp through the burned gas. The amplitude of the variations in radiation intensity depends on the absorptivity of the gas and on the intensity of the tungsten light source. From the observed amplitude, the absorptivity can be calculated; this is set equal to the emissivity of the gas in that wavelength interval (Kirchhoff's law). From the measured intensity of the hot gas radiation and this calculated emissivity, it is then possible to calculate the burned gas temperature. The details of the analysis required for application of the method and the assumptions made for its use in burner conditions are given, for example, in Ref. 9.

Data reduction following a firing test was accomplished by making deflection measurements of the prerun source calibration, and measuring the signal deflections from the photomultiplier and the pressure transducer over one or more cycles of oscillation at selected portions of the test. The number of temperature measurements over one cycle of pressure oscillation is determined by the chopping frequency of

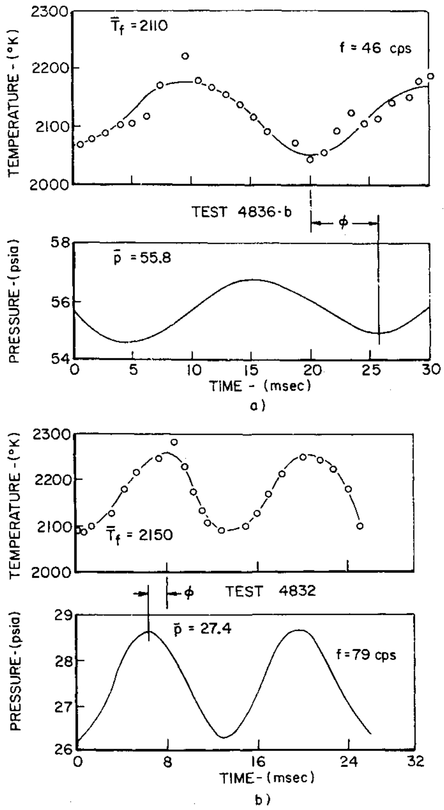


**Fig. 9 Temperature-pressure data for two different tests with the NWC burner.**

the disk, which was set to give approximately 20 such measurements per cycle. The gas temperature is then calculated with the relation[9]

$$T_g = \frac{c_2}{\lambda}\left[\ln\left\{\left(\frac{\Omega_2}{\Omega_1}\right)\left(\frac{D_1 - D_2}{D_3}\right)(e^{c_2/\lambda T_L} - 1) + 1\right\}\right]^{-1} \quad (12)$$

where $T_L$ = brightness temperature of lamp (constant for each test); $\lambda$ = 5893 a.u., sodium D line wavelength (average); $c_2$ = second radiation constant (1.438 cm °K); $\Omega_1/\Omega_2$ = ratio of solid angle of radiation from the lamp as it enters the collimating lens of the monochromator to solid angle of radiation from the radiating specie in gas; and $D_1$, $D_2$, $D_3$ = deflections caused by the flux from the tungsten comparison lamp, the comparison lamp shining through the flame, and the flame, respectively.

This optical technique for temperature measurement turned out to be fairly accurate; steady-state flame temperatures measured in the early part of firing, before strong oscillations set in, were typically within 2% of the theoretical adiabatic flame calculations. There are several burner conditions, however, that produce errors in the measurement of temperature. One is the accumulation of carbon on the quartz windows, representing a growth in absorptivity during the run that cannot be equated to gas emissivity. A second is nonuniformity both temporally and spatially of the burned gas temperature, since a composite propellant is not a uniform mixture but a statistically random one. A third stems from the great difficulty in dispersing uniformly tiny quantities of NaCl in the propellant mix.

Typical plots of temperature-pressure data are shown in Figs. 9a and 9b for two different propellants. Phase differences are indeed observed at these lower frequencies.

Data from selected tests appear in Table 1. Columns a–h represent experimental data; columns i and j are computed temperature fluctuations that will be discussed in some detail below. Alphabetical suffixes to the test number are used to identify the portion of the test record from which the data were taken. The time at which the data were taken appears in column a and is the time elapsed after ignition. Frequency was determined (column b) by measurement of the oscillograph record while the pressure and temperature data were obtained from plots similar to those shown in Fig. 9. Column g was calculated by taking the ratio of pressure oscillation amplitude to the mean pressure. The phase between temperature and pressure (column h) was noted from the pressure-temperature plots (as in Fig. 9).

## IV. Comparison of Experimental Results with Theoretical Expectations

In general, the tabulated pressure-temperature data show quite a diversity of behavior. The A-152 data represent the most comprehensive compilation of information available at present, but the question of whether the data fit a consistent pattern must await completion of more experiments.

A question of interest in the theory of oscillation burning can be answered immediately by direct inspection of the data in Table 1, namely, whether the temperature at the edge of the flame zone responds isentropically (with zero phase lags) to the pressure. For this purpose we can select the tests with large amplitudes of temperature oscillation above 40 cps, which demonstrate the point most accurately. The assumption that isentropicity is maintained at the flame edge leads to the calculated amplitudes of temperatures of column i based on $\gamma$ = 1.25: comparison with the measured ampli-

**Table 1 Pressure-temperature data**

| | | | | Pressure | | Temperature | | | | | |
|---|---|---|---|---|---|---|---|---|---|---|---|
| Propellant type | Test no. | Time $t$, sec [a] | Freq $f$,[a] cps [b] | Mean $p$, psia [c] | Oscillation amplitude, psi p-p [d] | Mean $\bar{T}$, °K [e] | Oscillation amplitude, $K$ p-p [f] | Severity of pressure oscillation $\Delta P$ [g] | Phase[b] $\phi$ fraction of cycle [h] | $\bar{T}\cdot\frac{\gamma-1}{\gamma}\Delta P$, °K p-p [i] | $S\Delta P$,[c] °K p-p [j] |
| PU | 4826A | 3.81 | 15.0 | 46.5 | 4.95 | 2064 | 44 | 0.106 | 0.078 | 43.8 | 70.7 |
| | 4829B | 2.70 | 37.0 | 53.7 | 5.25 | 2220 | 100 | 0.098 | −0.007 | 43.4 | 75.0 |
| A-152 | 4825A | 2.30 | 14.6 | 44.0 | 10.0 | 2008 | 190 | 0.227 | −0.415 | 91.2 | 48.5 |
| | 4825B | 2.60 | 14.6 | 46.5 | 9.0 | 1980 | 155 | 0.194 | −0.465 | 76.8 | 43.7 |
| | 4836C | 2.73 | 46.0 | 55.95 | 1.97 | 2120 | 120 | 0.039 | 0.026 | 16.4 | 9.55 |
| | 4836B | 3.38 | 46.0 | 50.80 | 2.20 | 2110 | 120 | 0.039 | 0.262 | 16.6 | 10.67 |
| | 4837B | 2.26 | 52.5 | 68.0 | 1.23 | 2130 | 135 | 0.018 | 0.105 | 7.70 | 5.97 |
| A-13 | 4832A | 2.88 | 81.0 | 26.7 | 1.3 | 2188 | 100 | 0.049 | −0.062 | 21.3 | ... |
| | 4832B | 3.18 | 78.7 | 27.5 | 2.4 | 2165 | 165 | 0.087 | −0.061 | 37.8 | ... |

[a] Time at which data was taken.
[b] Phase of temperature fluctuation relative to the pressure fluctuation. Negative sign indicates a temperature lag.
[c] $S$ = sensitivity of temperature to pressure: $S$ = 14.3°K/psi for PU propellant and $S$ = 4.85°K/psi for A-152 propellant.

tudes in column f shows that isentropicity does not hold. Furthermore, values of the phase lag between temperature and pressure, obtained by projecting backward from the point of observation to the flame edge, are −80°, −12°, and +55°, in tests 4832, 4837, and 4836.

It is evident, therefore, that the entropy at the edge of the flame oscillates with time. This same oscillation is preserved in the gas stream as it passes the point of observation. One can calculate the entropy variation by Eq. (5), with $T$ and $p$ taken from data such as given in Fig. 9.

Another facet of the temperature oscillations was considered, namely the effect of a flame temperature dependency on steady-state pressure. It is noted, in comparing mean temperature and mean pressure from PU and A-152 data, that at these relatively low rocket pressures, the temperature is a moderately strong function of pressure at these low-pressure burner conditions. This implies that the heat release in the gas phase is a function of pressure and that this must be added to the theoretical temperature fluctuations arising from the lag in the solid phase. Assuming, therefore, that this component of the temperature oscillation follows the pressure oscillations in the steady-state manner as measured and tabulated in Table 1, one can assign a sensitivity of temperature to pressure that can be used to compute this component of the temperature oscillation. Computations based on these assumptions are entered in column j of Table 1 and the temperature sensitivity for the two propellants appears in a footnote in that table. Comparison of the observed and computed temperature amplitudes based only on this effect indicate clearly a large disparity in some cases. Therefore, the steady-state temperature sensitivity to pressure does not offer an adequate explanation by itself of the large temperature oscillations observed at the higher frequencies. Also, there can be no phase difference at the flame edge if this were the only phenomenon.

It seems appropriate then to compare the experimental temperature fluctuations with the analytical predictions for unsteady burning given in Eqs. (4–11). With the KTSS model to describe the dynamic flame temperature response,** the theoretical relation given by Eq. (11) does indeed offer an adequate explanation of the large amplitude temperature oscillations observed at the testing frequencies. As demonstrated in Ref. 6, the surface temperature and the flame temperature fluctuations are maximum in the frequency range centering about the resonant frequency for the propellant. The tests described in Table 1 are definitely in the frequency range where, for appropriate values of $H$ and $m$, i.e., the combustion parameters introduced in the KTSS model, the fluctuations predicted are large enough to match those observed.

For comparison with the two typical experimental plots of temperature-pressure data shown in Figs. 9a and 9b, the theoretical temperature response curves were calculated from Eq. (11) using $H = 0.77$, $m = 6$, $n = 0.5$, and $\xi = 0.23$. Figure 10a shows this theoretical calculation for comparison with Fig. 9a made as close as possible to the same burner conditions of test 4836B. The predicted phase angle is 131° (lead) and the maximum temperature fluctuation $|T'(x,t)/\bar{T}_f|$ is calculated to be 0.0242. The experiment gives a lead of $\phi = 95°$ and $|T'(x,t)/\bar{T}_f| = 0.0284$. Similarly, comparison of test 4832 (Fig. 9b) to theory is made with the theoretical calculation given in Fig. 10b. The agreement this time was not as good; theoretically, the lead was 3.1° and the amplitude was 0.012, while the experimental values were 22° and 0.038, respectively.

At this point it should be mentioned, however, that due to the diversity of data described in Table 1, which comes about from nonideal burner conditions, such as flow reversal, transient heat loss to the walls, and those inherent errors in

** This model is chosen over others since it describes the diffusion flame structure of composite AP solid propellants.

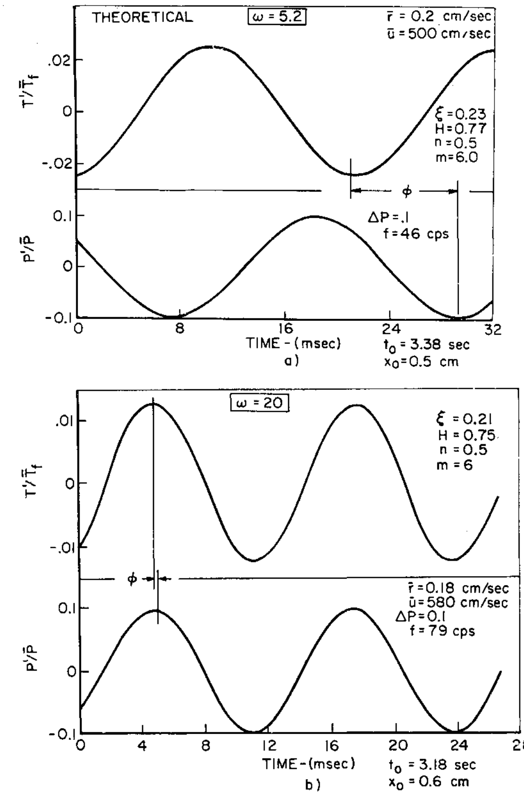


**Fig. 10 Theoretical calculation of temperature response to oscillation pressure at observation distance the same as test 4836b and 4832, respectively, i.e., those shown in Fig. 9.**

the measurement of temperature discussed in Sec. III, the comparison of all the data with theory is not made here. The variance is typical to the two aforementioned cases. More data is needed, with systematic variation of propellants and burner conditions (as discussed below) to select one model exclusively over another. However, the fact that entropy waves were observed and their behavior can be qualitatively described by a combustion model with realistic parameters is of significance.

## V. Conclusion

On the basis of measurements of burned gas temperature in the stream flowing from the flame of a burning solid propellant, waves of entropy have been found at the same frequency at the pressure oscillation in the combustor. These entropy waves are proof of the existence of entropy oscillations at the edge of the flame zone during oscillatory burning. Although part of this entropy oscillation may be attributed to the in-phase oscillation of heat release in the gaseous part of the combustion wave due to the pressure sensitivity to the reaction, the largest part of the entropy oscillation appears to be due to the lag of the thermal wave in the subsurface domain of the solid.

The latter effect has been the subject of various theoretical papers in the past, based on various physical-chemical models of the combustion wave. The entropy fluctuations observed in the experiments reported in this paper are generally in agreement, both in phase and in magnitude, with the predictions of the KTSS model, although at this time the data are not extensive enough to exclude all other theories.

In fact, there are several models, some of which have current reference value, that predict flame temperature oscillations that provide entropy waves. One of these is the model by Denison and Baum,[7] and its prediction of the amplitude of the entropy wave as a function of frequency is shown in Fig. 1, along with the predictions of the KTSS model.[6] Both models seem to predict similar behavior. For example, each displays a minimum in the entropy wave amplitude vs frequency that corresponds to the reciprocal of the solid-phase (thermal) wavetime.

However, on closer inspection, the similarity breaks down. From the definition of the combustion parameters that influence the amplitude of the oscillation of the dynamic burning rate and the flame temperature, it can be shown that the two models lead to opposite predictions as to variation of amplitude of the entropy wave in the burned gas as the composition of the propellant is altered. Since $n$ in the KTSS model corresponds to $N/2$ in the DB model and $m$ to $A$, it can be seen that the KTSS model predicts a decrease in entropy amplitude as $H$ increases, whereas the DB model predicts a similar decrease in entropy amplitude as $1/\alpha$ increases. From the definition of the term $1/\alpha$ in Ref. 7, one can show that $1/\alpha$ increases as the oxidizer loading decreases, and therefore as the flame temperature decreases, whereas, as discussed in Ref. 6, $H$ increases as the oxidizer loading is *increased*. Thus, the two theories make opposite predictions as to the effect of changes in oxidizer content on entropy amplitude.

Therefore, in order to determine from the study of entropy which of these two models more closely describes the dynamic burning of solid propellants, a systematic study of several propellant formulations must be made in which the oxidizer loading is altered. This study has yet to be carried out, and it must be conceded, therefore, that at this time, the data are not sufficiently accurate to support one model exclusively against all others. However, it has definitely been shown at least that the KTSS model is consistent with the observations and that other theories resting on the assumption of constant entropy at the edge of the flame zone, such as that given in Ref. 12, must be declared incorrect.

## References


[1] Hart, R. H. and Cantrell, R. H., "Amplification and Attenuation of Sound by Burning Propellants," *AIAA Journal*, Vol. 1, No. 2, Feb. 1963, pp. 398–404.

[2] Horton, M. D., "Acoustic Admittance of a Burning Propellant Surface," *ARS Journal*, Vol. 32, No. 4, April 1962, pp. 644–646.

[3] Price, E. W., "Experimental Solid Rocket Combustion Instability," *Proceedings of the Tenth Symposium (International) on Combustion*, The Combustion Institute, 1965, pp. 1067–1082.

[4] Culick, F. E. C., "A Review of Calculations for Unsteady Burning of a Solid Propellant," *AIAA Journal*, Vol. 6, No. 12, Dec. 1968, pp. 2241–2255.

[5] Waesche, R. H. W. and Summerfield, M., "Solid Propellant Combustion Instability: Oscillatory Burning of Solid Rocket Propellants," Rept. 751, Aug. 1965, Aerospace and Mechanical Sciences Dept., Princeton Univ., Princeton, N. J.

[6] Krier, H. et al., "Nonsteady Burning Phenomena of Solid Propellants: Theory and Experiments," *AIAA Journal*, Vol. 6, No. 2, Feb. 1968, pp. 278–285.

[7] Denison, M. R. and Baum, E., "A Simplified Model of Unstable Burning in Solid Propellants," *ARS Journal*, Vol. 31, No. 8, Aug. 1961, pp. 1112–1122.

[8] Steinz, J. A., Stang, P. L., and Summerfield, M., "The Burning Mechanism of Ammonium Perchlorate-Based Composite Propellants," AIAA Paper 68-658, Cleveland, Ohio, 1968.

[9] Krier, H., "Solid Propellant Burning in Nonsteady Fields," Ph.D. thesis, Sept. 1968, Aerospace and Mechanical Sciences Dept., Princeton Univ.

[10] T'ien, J. S., Sirignano, W. A., and Summerfield, M., "Theory of $L^*$ Combustion Instability with Temperature Oscillations," AIAA Paper 68-179, New York, 1968; also *AIAA Journal*, to be published.

[11] Mathes, H. B., "Experimental Techniques in Low Frequency Solid Propellant Acoustic Instability," *Proceedings of the 3rd ICRPG Combustion Conference*, CPIA Publication 138, Vol. 1, Feb. 1967, pp. 237–251.